Identification of a novel mannose-capped lipoarabinomannan from *Amycolatopsis sulphurea*

Kevin J. C. GIBSON*†, Martine GILLERON‡, Patricia CONSTANT‡, Germain PUZO‡, Jérôme NIGOU*‡ and Gurdyal S. BESRA†[1]

*Department of Microbiology and Immunology, University of Newcastle, Newcastle-upon-Tyne NE2 4HH, U.K., †School of Biosciences, The University of Birmingham, Edgbaston, Birmingham B15 2TT, U.K., and ‡Department of Molecular Mechanisms of Mycobacterial Infections, Institut de Pharmacologie et de Biologie Structurale, CNRS, UMR 5089, 205 route de Narbonne, 31077 Toulouse cedex 4, France

The genus *Amycolatopsis* is a member of the phylogenetic group nocardioform actinomycetes, which also includes the genus *Mycobacterium*. Members of this group have a characteristic cell envelope structure, dominated by various complex lipids and polysaccharides. Amongst these, lipoglycans are of particular interest since mycobacterial lipoarabinomannans are important immunomodulatory molecules. In this study we report the isolation and structural characterization of *Amycolatopsis sulphurea* lipoarabinomannan, designated AsuLAM. SDS/PAGE analysis revealed that AsuLAM was of an intermediate size between *Mycobacterium tuberculosis* lipoarabinomannan and lipomannan, confirmed by matrix-assisted laser-desorption ionization–time-of-flight mass spectrometry that predicted an average molecular mass of 10 kDa. Using a range of chemical degradations, NMR experiments and capillary electrophoresis analysis, AsuLAM was revealed as an original structure. The mannosyl-phosphatidyl-*myo*-inositol anchor exhibits a single acyl-form, characterized by a diacylated glycerol moiety, and contains, as one of the main fatty acids, 14-methyl-pentadecanoate, a characteristic fatty acid of the *Amycolatopsis* genus. AsuLAM also contains a short mannan domain; and is dominated by a multi-branched arabinan domain, composed of an ($\alpha 1 \rightarrow 5$)-Ara*f* (arabinofuranose) chain substituted, predominately at the *O*-2 position, by a single β-Ara*f*. The arabinan domain is further elaborated by manno-oligosaccharide caps, with around one per molecule. This is the first description of manno-oligosaccharide caps found in a non-mycobacterial LAM. AsuLAM was unable to induce the production of the pro-inflammatory cytokine tumour necrosis factor α when tested with human or murine macrophage cell lines, reinforcing the paradigm that mannose-capped LAM are poor inducers of pro-inflammatory cytokines.

Key words: actinomycetes, capillary electrophoresis, lipoglycan, MALDI-TOF-MS, NMR, TNF-α.

INTRODUCTION

The potential virulence of atypical actinomycetes, such as *Amycolatopsis* strains, is well documented with the reported isolation of *Amycolatopsis orientalis* from human and animal sources [1,2]. In addition, *Amycolatopsis* sp MJ126-NF4 [3] and MK299-95F4 [4], which are close relations of *Amycolatopsis sulphurea*, were shown to produce azicemicin and epoxyquinomicin antibiotics, respectively. Prior to the creation of the genus *Amycolatopsis*, such strains were classified within the genus *Nocardia*, which forms part of the phylogenetic group nocardioform actinomycetes [5]. In common with members of this phylogenetic group, *Amycolatopsis* species are Gram positive, non-sporulating and partially acid-fast [6]. This group also includes such genera as *Mycobacterium*, *Tsukamurella* and *Corynebacterium*. Moreover, members of this group have a characteristic cell envelope structure, composed primarily of branched long-chain lipids termed mycolic acids [7]. In contrast to this group, *Amycolatopsis* strains do not contain any mycolic acids, which led Lechevalier et al. [5] to propose a new genus, *Amycolatopsis*, aptly describing these strains lacking the signature mycolic acids.

Research efforts in mycobacterial cell envelope architecture have revealed an abundance of complex lipoglycans, such as phosphatidyl-*myo*-inositol mannosides (PIMs), lipomannan (LM) and lipoarabinomannan (LAM) [7]. Mycobacterial LAM is a large heterogeneous macroamphiphile that possesses three distinct domains: a carbohydrate backbone, a mannosyl-phosphatidyl-*myo*-inositol (MPI) anchor and various capping motifs [8–10]. The carbohydrate backbone comprises two homopolysaccharides, D-mannan and D-arabinan. In all species described to date, the D-mannan domain exists as a linear $\alpha(1 \rightarrow 6)$-Man*p* backbone substituted according to the species at the *O*-2 or *O*-3 positions by single Man*p* residues. The D-arabinan domain consists of a linear $\alpha(1 \rightarrow 5)$-Ara*f* (arabinofuranose) backbone punctuated by branching fashioned from 3,5-*O*-linked α-D-Ara*f* residues [8–10].

Comparative analyses of LAMs from different mycobacterial strains have shown that within this common structure there lies a great deal of heterogeneity, including variations in the acylation states of the MPI anchor [11], the presence of succinate [12] and methylthiopentose sugar residues [13], and capping motifs decorating the non-reducing termini of the Ara*f* residues. In slow-growing mycobacteria, such as *M. tuberculosis*, these motifs consist of mannopyranose (Man*p*) residues [14,15]; whereas

Abbreviations used: Ara*f*, arabinofuranose; APTS, 1-aminopyrene-3,6,8-trisulphonate; AsuLAM, *Amycolatopsis sulphurea* lipoarabinomannan; CE-LIF, capillary electrophoresis-laser-induced fluorescence; δ, chemical shift; 1D, one-dimensional; 2D, two-dimensional; HMQC, heteronuclear multiple quantum correlation spectroscopy; HOHAHA, homonuclear Hartmann–Hahn spectroscopy; IFN, interferon; IL, interleukin; LAM, lipoarabinomannan; LM, lipomannan; MALDI-TOF, matrix-assisted laser-desorption ionization–time-of-flight; Man*p*, mannopyranose; ManLAM, LAM with mannosyl caps; MPI, mannosyl-phosphatidyl-*myo*-inositol; PILAM, LAM with phosphoinositide caps; PIM, phosphatidyl-*myo*-inositol mannoside; ReqLAM, *Rhodococcus equi* lipoarabinomannan; t, terminal; TFA, trifluoroacetic acid; TLR, toll like receptor; TMS, trimethyl-silyl; TNF-α, tumour necrosis factor α.

[1] To whom correspondence should be addressed (email g.besra@bham.ac.uk).

fast-growing mycobacteria, such as *Mycobacterium smegmatis*, possess phospho-inositol residues [16,17], resulting in LAM being termed either ManLAM or PILAM, respectively. These subtle differences in the capping motifs are thought to explain the different immunomodulatory functions of ManLAM and PILAM. ManLAMs possess the ability to inhibit the production of pro-inflammatory cytokines such as interleukin (IL)-12 and tumour necrosis factor (TNF)-α [18,19]; conversely, PILAM stimulates the production of these pro-inflammatory cytokines [17,20]. These facts not only corroborate the findings that slow-growing mycobacteria have the ability to exist and multiply within phagocytic cells and fast-growing mycobacteria do not, but illustrate also the great importance of ManLAM as a key virulence factor, enabling the persistence of slow-growing mycobacteria within phagocytic cells [21].

Lipoglycans structurally related to mycobacterial LAM have been identified in a number of other actinomycetes, including *Corynebacterium matruchotii* [22], *Dietza maris* [23], *Gordonia rubropertincta* [24] and *Rhodococcus rhodnii* [25]. However, these studies did not demonstrate whether these lipoglycans possessed *in vitro* biological activity. Recently, Garton et al. [26] described the structure of a novel lipoglycan from *Rhodococcus equi* (ReqLAM). They demonstrated that the purified lipoglycan had the ability to induce an immune response in equine macrophages that was very similar to that induced by virulent *R. equi*, suggesting that the early macrophage cytokine responses to the bacteria can be attributed to this novel ReqLAM [26].

In this study we report the isolation and characterization of a mannose-capped LAM originating from a non-mycolate, non-mycobacterial strain and discuss the relationship between this novel structure and its ability to induce inflammatory responses.

MATERIALS AND METHODS

Bacteria and growth conditions

A. sulphurea was purchased from the DSMZ ('German Collection of Microorganisms and Cell Cultures', Braunschweig, Germany), strain DSM 46092. It was routinely grown at 30 °C in GYM streptomyces medium (4 g/litre glucose, 4 g/litre yeast extract, 10 g/litre maltose extract, and 0.05 % Tween 80). Cells were grown to late log phase and harvested by centrifugation for 15 min at 18 000 **g**, followed by washing (supernatent was removed and then cells were resuspended in deionized water and centrifuged again as above). The washed cells were then freeze-dried using an Edwards freeze-dryer Modulyo machine.

Purification of *Amycolatopsis sulphurea* lipoarabinomannan (AsuLAM)

Purification procedures were adapted from protocols established for the extraction and purification of mycobacterial lipoglycans [27,28]. Briefly, the cells were delipidated at 60 °C by mixing in chloroform/methanol (1:1, v/v) overnight. The organic extract was removed by filtration and the delipidated biomass was resuspended in deionized water and disrupted by sonication on ice using an MSE Soniprep (MSE, Crawley, Surrey, U.K.) at 12 micro amplitude, 60 s on, 90 s off for 10 cycles. The cellular glycans and lipoglycans were further extracted by refluxing the broken cells in 50 % ethanol at 65 °C overnight. Contaminating proteins were removed by enzymic degradation using α-amylase and protease treatments followed by dialysis. The resulting extract was resuspended in buffer A (15 % propan-1-ol in 50 mM ammonium acetate), loaded onto an octyl-Sepharose CL-4B column (Sigma; 50 cm × 2.5 cm), and eluted with 400 ml of buffer A at 5 ml/h, enabling the removal of non-lipidic moieties [18]. The retained lipoglycans were eluted with 400 ml of buffer B (50 % propan-1-ol in 50 mM ammonium acetate). The resulting lipoglycans were resuspended in buffer C [0.2 M NaCl, 0.25 % (w/v) sodium deoxycholate, 1 mM EDTA and 10 mM Tris/HCl, pH 8], to a final concentration of 200 mg/ml and loaded onto a Sephacryl S-200 HR column (Sigma; 50 cm × 2.5 cm) and eluted with buffer C at a flow rate of 5 ml/h. Fractions (1.25 ml) were collected and analysed by SDS/PAGE (15 % gel) followed by periodic acid-silver nitrate staining. The resulting lipoglycan fractions were pooled, dialysed extensively against water, freeze-dried and stored at −20 °C. The yield of AsuLAM was 0.7 % (w/w).

Matrix-assisted laser-desorption ionization–time-of-flight mass spectrometry (MALDI-TOF-MS)

The matrix used was 2,5-dihydroxybenzoic acid at a concentration of 10 μg/μl, in a mixture of water/ethanol (1:1, v/v). Aliquots (0.5 μl) of AsuLAM, at a concentration of 10 μg/μl, were mixed with 0.5 μl of the matrix solution. Analyses were performed on a Voyager DE-STR MALDI-TOF instrument (PerSeptive Biosystems, Framingham, MA, U.S.A.) using linear mode detection. Mass spectra were recorded in the negative mode using a 300 ns time delay with a grid voltage of 94 % of full accelerating voltage (20 kV) and a guide wire voltage of 0.1 %. The mass spectra were mass assigned using external calibration.

Fatty-acid analysis

AsuLAM (200 μg) was deacylated using strong alkaline hydrolysis (200 μl of 1 M NaOH at 110 °C for 2 h). The reaction mixture was neutralized with HCl and the liberated fatty acids were extracted three times with chloroform and, after drying under nitrogen, they were methylated using three drops of 10 % (w/w) BF_3 in methanol (Fluka, Gillingham, Dorset, U.K.) at 60 °C for 5 min. The reaction was stopped by the addition of water, and the fatty acid methyl esters were extracted three times with chloroform. After drying, the fatty acid methyl esters were solubilized in 10 μl of pyridine and trimethylsilylated using 10 μl of hexamethyldisilazane and 5 μl of trimethylchlorosilane at 25 °C for 15 min. After drying under a stream of nitrogen, the fatty acid derivatives were solubilized in cyclohexane before analysis by GLC and GLC-MS.

Glycosidic-linkage analysis

Glycosyl linkage composition was performed according to the modified procedure from Ciucanu and Kerek [29]. The per-*O*-methylated AsuLAM was hydrolysed using 500 μl of 2 M trifluoroacetic acid (TFA) at 110 °C for 2 h, reduced using 350 μl of a 10 mg/ml solution of $NaBD_4$ (1M ammonium hydroxide/ethanol; 1:1, v/v) and per-*O*-acetylated using 300 μl of acetic anhydride for 1 h at 110 °C. The resulting alditol acetates were solubilized in cyclohexane before analysis by GLC and GLC-MS.

1-Aminopyrene-3,6,8-trisulphonate (APTS) derivatization and capillary electrophoresis

AsuLAM (1 μg) was hydrolysed using either strong acid hydrolysis (30 μl of 2 M TFA at 110 °C for 2 h) or mild partial acid hydrolysis (30 μl of 0.1 M HCl at 110 °C for 20 min). The samples were dried and mixed with 0.3 μl of 0.2 M APTS

(Interchim, Montluçon, France) in 15 % acetic acid and 0.3 μl of a 1 M sodium cyanoborohydride solution dissolved in tetrahydrofuran. The reaction mixture was heated to 55 °C for 90 min and subsequently quenched by the addition of 20 μl of water. A 2 μl solution of the APTS-derivatized solution was diluted 10-fold before being subjected to capillary electrophoresis. Analyses were performed on a P/ACE capillary electrophoresis system (Beckman Instruments, Inc., Spinco Division, Palo Alto, CA, U.S.A.) with the cathode on the injection side and the anode on the detection side (reverse polarity). The electropherograms were acquired and stored on a Dell XPS P60 computer using the System Gold software package (Beckman Instruments, Inc.). APTS derivatives were loaded by applying 0.5 psi (3.45 kPa) vacuum for 5 s (6.5 nl injected). Separations were performed using an uncoated fused-silica capillary column (Sigma, Division Supelco, Saint-Quentin-Fallavier, France) of 50 μm internal diameter with 40 cm effective length (47 cm total length). Analyses were carried out at 25 °C with an applied voltage of 20 kV using acetic acid 1 % (w/v) and 30 mM triethylamine in water, pH 3.5 as running electrolyte. The detection system consisted of a Beckman laser-induced fluorescence (LIF) equipped with a 4-mW argon-ion laser with the excitation wavelength of 488 nm and emission wavelength filter of 520 nm.

NMR spectroscopy

NMR spectra were recorded on a Bruker (Karlsruhe, Germany) DMX-500 spectrometer equipped with a double resonance (^{1}H/X)-BBi z-gradient probe head. AsuLAM (5 mg) was exchanged in ^2H_2O (^{2}H, 99.97 % from Euriso-top, Saint-Aubin, France), with intermediate freeze-drying, then re-dissolved in 0.4 ml of ^2H_2O for ^{1}H, ^{1}H-^{1}H and ^{1}H-^{13}C experiments or in 0.4 ml of DMSO-d6 (^{2}H, 99.8 % from Euriso-top, Saint-Aubin, France) for ^{31}P and ^{1}H-^{31}P experiments, and analysed in 200 mm × 5 mm 535-PP NMR tubes. Data were processed on a Bruker-X32 workstation using the xwinnmr program. The one-dimensional (1D) proton (^{1}H) spectra were recorded at 308 K using a 90° tipping angle for the pulse and 1 s as recycle delay between each of the 256 acquisitions of 1.64 s. The spectral width of 4807 Hz was collected in 16 k complex points that were multiplied by a Gaussian function (LB = -1, GB = 0.1) prior to processing up to 32 k real points in the frequency domain. After Fourier transformation, the spectra were baseline-corrected with a fourth order polynomial function. The ^{1}H NMR chemical shifts were referenced relative to internal acetone at 2.225 p.p.m. The 1D ^{31}P spectrum was measured at 202.46 MHz at 343 K and phosphoric acid (85 %) was used as external reference (δ_P 0.0). The spectral width of 6188 Hz was collected in 16 k complex points that were multiplied by an exponential function (LB = -5 Hz) prior to processing to 32 k real points in the frequency domain. The scan number was 2048. Two-dimensional (2D) spectra were recorded without sample spinning, and data were acquired in the phase-sensitive mode using the time-proportional phase increment (TPPI) method. The 2D ^{1}H-^{13}C heteronuclear multiple quantum correlation (HMQC) and ^{1}H-^{31}P homonuclear Hartmann–Hahn spectroscopy (HMQC-HOHAHA) were recorded in the proton-detected mode with a Bruker 5-mm ^{1}H broad band tunable probe with reverse geometry. The globally optimized alterning-phase rectangular pulses ('GARP') sequence [30] at the carbon or phosphorus frequency was used as a composite pulse decoupling during acquisition. The ^{1}H-^{13}C HMQC spectrum was obtained according to Bax and Subramanian pulse sequence [31]. Spectral widths of 25154 Hz in ^{13}C and 4807 Hz in ^{1}H dimensions were used to collect a 2048 × 512 (TPPI) point data matrix with 52 scans/t1 value expanded to 4096 × 1024 by zero filling. The relaxation delay was 1 s. A sine bell window shifted by $\pi/2$ was applied in both dimensions. ^{1}H-^{31}P HMQC-HOHAHA spectrum was obtained using the Lerner and Bax pulse sequence [32]. Spectral widths of 4049 Hz in ^{31}P and 4496 Hz in ^{1}H dimensions were used to collect a 2048 × 100 (TPPI) point data matrix with 64 scans/t1 value expanded to 4096 × 1024 by zero filling. The relaxation delay was 1 s. A sine bell window shifted by $\pi/2$ was applied in both dimensions. The 2D ^{1}H-^{1}H HOHAHA spectrum was recorded using a MLEV-17 mixing sequence of 112 ms [33]. The spectral width was 4807 Hz in the F_2 dimension and 4223 Hz in the F_1 dimension. 512 Spectra of 4096 data points with 24 scans/t1 increment were recorded.

TNF-α production by macrophages

THP-1 and J774 monocyte/macrophage human and murine cell lines, respectively, were maintained in continuous culture with RPMI 1640 medium (Life Technologies, Paisley, Renfrewshire, Scotland, U.K.), plus 10 % fetal calf serum (Life Technologies) in an atmosphere of 5 % CO_2 at 37 °C; THP-1 as non-adherent and J774 as adherent cells. Purified AsuLAM was added in duplicate to monocyte/macrophage cells (5×10^5 cells/well) in 24-well culture plates and then incubated for 6 h at 37 °C. Stimuli were previously incubated for 1 h at 37 °C in the presence or absence of 10 μg/ml polymyxin B (Sigma), known to inhibit the effect of contaminating lipopolysaccharide [20]. The assays were conducted independently and in triplicate. Supernatants were assayed for TNF-α using the previously described cytotoxic assay against WEHI164 clone 13 cells [34]. Basically, 50 μl of supernatant was added to 50 μl of WEHI cells (5×10^5 cells/ml) in flat-bottom 96-well plates and incubated for 20 h at 37 °C, then 50 μl of tetrazolium salts (MTT, 1 mg/ml in PBS) were added to each well and incubated for 4 h. Formazan crystals were solubilized with 100 μl of lysis buffer (*N*,*N*-dimethylformamide, 30 % SDS (1:2) adjusted to pH 4.7 with acetic acid) and the optical density read at 570 nm with an ELISA plate reader (Bio-Tek Instruments, Neufahrn, Germany). The TNF-α content of the supernatants was estimated using a reference curve obtained by measuring serial dilutions of human recombinant TNF-α (Life Technologies). Lipopolysaccharide was from *Escherichia coli* 055:B5 (Sigma) and ManLAM from *Mycobacterium bovis* BCG.

RESULTS

Purification and general structural features

A. sulphurea lipoglycan was purified by the methods previously reported for mycobacterial lipoglycans [27,28]. The following critical steps were performed: (i) ethanol/water extraction of the lipoglycans from disrupted and delipidated cells, (ii) enzymic degradation of contaminants, (iii) separation of lipoglycans from glycans by hydrophobic-interaction chromatography, and (iv) size fractionation of lipoglycans by gel-permeation chromatography. The procedure allowed the recovery of a lipoglycan with a size intermediate between *M. tuberculosis* LAM and LM, as visualized by SDS/PAGE analysis (Figure 1A). The negative MALDI-TOF mass spectrum of the lipoglycan exhibited a broad unresolved peak centred at *m*/*z* 10200, indicating a molecular mass of around 10 kDa for the major molecular species (Figure 2). The lipoglycan was subsequently subjected to total acid hydrolysis (2 M TFA for 2 h at 110 °C) followed by either APTS or trimethyl-silyl (TMS) derivatization in the presence of

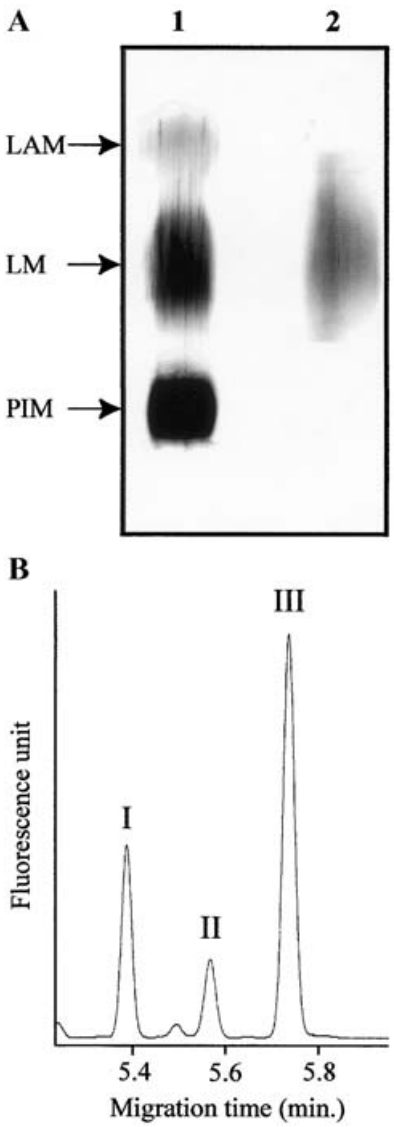

Figure 1 SDS/PAGE (A) and CE-LIF (B) analyses of *A. sulphurea* lipoglycan

(**A**) Lane 1, *M. tuberculosis* ManLAM, LM and PIM (top, medium and bottom bands, respectively); lane 2, *A. sulphurea* lipoglycan. (**B**) Lipoglycan (1 μg) and 1 nmol mannoheptose were hydrolysed using 30 μl of 2 M TFA, for 2 h at 110 °C, dried, APTS derivatized and subjected to CE-LIF. CE analysis was carried out with a 470 mm $\times$ 50 μm capillary, at a temperature of 20 °C, with an applied voltage of 20 kV and monitored by LIF. 1 % (w/v) Acetic acid and 30 mM triethylamine, pH 3.5, was used as running electrolyte. I, Ara-APTS; II, Man-APTS; III, mannoheptose-APTS (internal standard).

mannoheptose as an internal standard. The APTS derivatives were analysed by capillary electrophoresis monitored by laser-induced fluorescence (CE-LIF). The electropherogram (Figure 1B) showed three peaks assigned, due to the co-injection of authentic standards, as Ara-APTS (I), Man-APTS (II) and mannoheptose-APTS (III). The relative composition of the lipoglycan polysaccharide backbone, from peak integration, was determined as 73 % Ara and 27 % Man. In addition to Ara and Man, TMS derivatives analysed by GLC-MS revealed the presence of glycerol and inositol (results not shown). The presence of fatty acids was investigated by alkaline hydrolysis followed by GLC-MS analysis of fatty acid methyl esters (results not shown). The predominant fatty acid methyl esters recovered were methyl palmitate ($C_{16:0}$) (38 %) and its isomer, with a faster elution

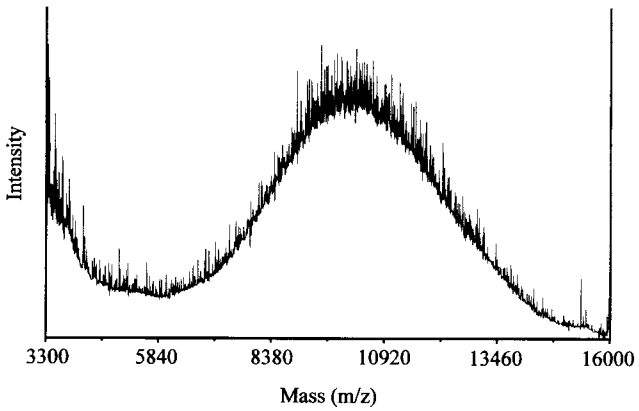

Figure 2 MALDI-TOF-MS analysis of *A. sulphurea* lipoglycan

An aliquot (0.5 μl) of a 10 μg/μl *A. sulphurea* lipoglycan solution was mixed with 0.5 μl of the matrix solution [10 μg/μl 2,5-dihydroxybenzoic acid in ethanol/water (1:1, v/v)] and analysed by MALDI-TOF-MS in the negative mode.

time, methyl 14-methyl-pentadecanoate (24 %). Identification of methyl 14-methyl-pentadecanoate in AsuLAM was in agreement with the presence of this fatty acid within the *Amycolatopsis* genus [35]. In addition, methyl pentadecanoate (7 %), methyl n-heptadecanoate (15 %), two branched methyl heptadecanoate isomers (5 % and 3 %), methyl octadecenoate ($C_{18:1}$) (1 %), methyl stearate ($C_{18:0}$) (5 %), and methyl tuberculostearate (methyl 10-methyloctadecanoate, $C_{19:0}$) (2 %) were present in smaller amounts.

In summary, the presence of Ara (73 %) and Man (27 %), as well as glycerol, inositol and fatty acids, the basic components of a phosphatidyl-*myo*-inositol anchor, provided the first indications of a lipoglycan with a structure related to mycobacterial LAM. The lipoglycan was subsequently termed AsuLAM.

Carbohydrate backbone

The glycosidic linkages present in AsuLAM were analysed by per-*O*-methylation analysis. The partially per-*O*-methylated, per-*O*-acetylated alditols, identified by GLC-MS, were terminal (t)-Ara*f* and 2,5-Ara*f*. In addition, 2-Ara*f*, 5-Ara*f*, t-Man*p*, 6-Man*p*, 2-Man*p*, 2,6-Man*p* and 3,6-Man*p* residues were found in smaller proportions.

Arabinan domain

CE-LIF and per-*O*-methylation analysis data converged, enabling us to establish that the major domain of the AsuLAM molecule was composed of Ara residues. This domain was subsequently analysed by NMR. The ^{1}H-NMR anomeric region of AsuLAM was composed of several signals with different intensities (Figure 3A). The anomeric region of the ^{1}H-^{13}C HMQC NMR spectrum (Figure 3B) revealed a number of signals overlapped in the ^{1}H dimension, revealing many more spin systems than those observed from the 1D ^{1}H NMR spectrum. Indeed, the anomeric area of the ^{1}H-^{13}C HMQC NMR spectrum is dominated by two intense cross peaks at δ_{H1}/δ_{C1} 5.18/108.7 (I_1) and δ 5.15/103.4 (II_1) and several weaker signals at δ_{H1}/δ_{C1} 5.09/110.2 (III_1), 5.30/101.9 (IV_1), δ 5.08/102.9 (V_1), 5.18/97.8 (VI_1) and 5.15/97.8 (VII_1). From their high intensity, spin systems I and II were likely to be the major units identified by per-*O*-methylation analysis, 2,5-Ara*f* and t-Ara*f*. The ^{1}H and ^{13}C resonances of spin systems I and II

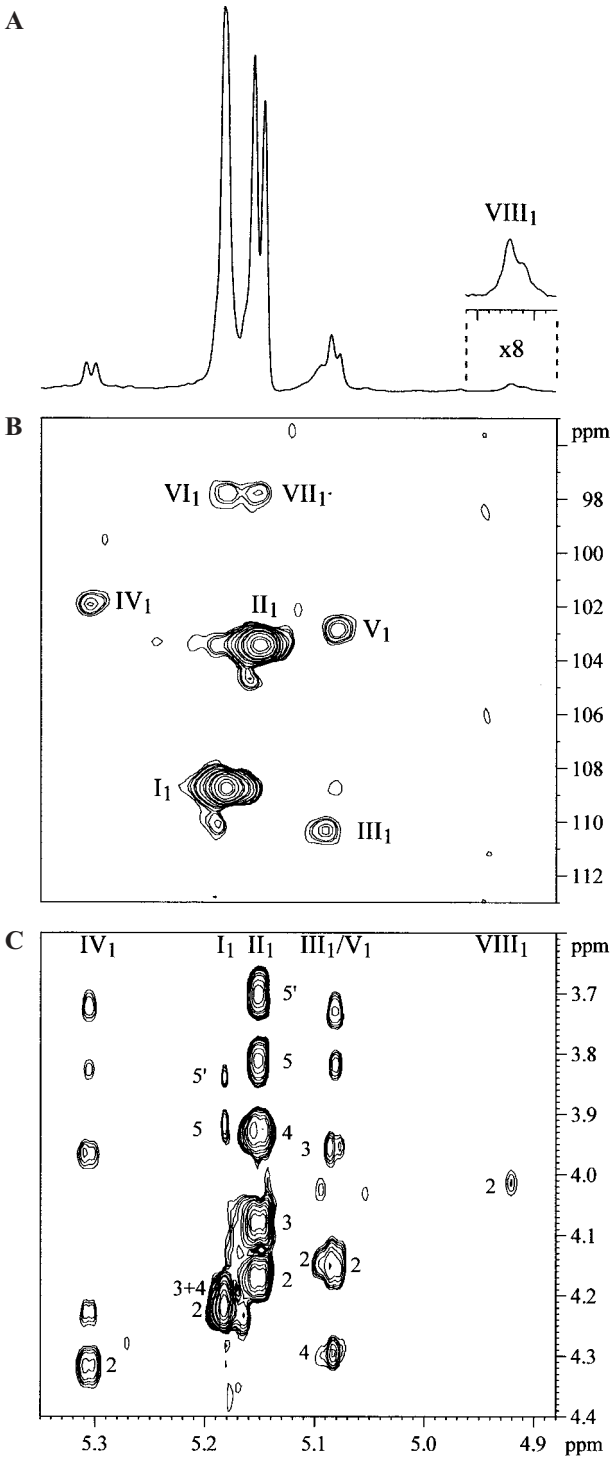

Figure 3 1D ^{1}H (A) and 2D ^{1}H-^{13}C HMQC (B) ^{1}H-^{1}H HOHAHA τ_m 112 ms (C) spectra of AsuLAM in ^2H_2O at 308 K

Expanded regions (δ ^{1}H: 4.88–5.35) (**A**) and (δ ^{1}H: 4.88–5.35, δ ^{13}C: 95–113) (**B**) are shown. Glycosyl residues are labelled in roman numerals, and their carbons and protons in Arabic numerals. I, 2,5-α-Ara*f*; II, t-β-Ara*f*; III, 5-α-Ara*f*; IV and V, β-Ara*f*; VI and VII, α-Man*p*; VIII, 6-α-Man*p*.

were assigned from ^{1}H-^{13}C HMQC and ^{1}H-^{1}H HOHAHA NMR experiments (partially shown in Figures 3B and 3C) and based on our previous studies with mycobacterial LAM [15,17,36], with assignments summarized in Table 1. Resonances I and II correspond to 2,5-Ara*f* and t-Ara*f* units, and were unambiguously assigned as 2,5-α-Ara*f* and t-β-Ara*f* respectively, according to the following lines of evidence. The β-anomeric configuration of t-β-Ara*f* (II) was based on its C-1 chemical shift at δ 103.4 compared with α/β-Ara*f* units in mycobacterial LAM (αAra*f*: δ_{C-1} 108–110; βAra*f*: δ_{C-1} 103) [15,17], with the chemical shift of the C-4 carbon at 84.8 p.p.m. (Table 1) confirming a furanose ring form. Also C-2, C-3 and C-5 resonances (Table 1) were not deshielded, which are in agreement with an unsubstituted β-Ara*f* unit. The α-anomeric configuration of 2,5-α-Ara*f* (I) was based on its C-1 chemical shift at δ 108.7. Glycosylation at position 5 was shown through the deshielding of the C-5 resonance at δ 69.2 (Table 1) as compared with the C-5 resonance of the unsubstituted t-β-Ara*f* at δ 65.8 ($\Delta\delta$ 3.4 p.p.m.). Glycosylation at position 2 was determined by the deshielding of its C-2 resonance at δ 89.5 (Table 1) as compared with the C-2 resonance of t-β-Ara*f* (I) at δ 79.1 ($\Delta\delta$ 10.4 p.p.m.). Due to their weak intensity, the remaining minor spin systems, corresponding to around 1 unit per molecule, could not be fully attributed. Spin system III was characterized by δ_{C1} at 110.2 (III_1, Figure 3b) and was assigned as an α-Ara*f*, with δ_{C1} and δ_{C2} at 110.2 and 83.7 respectively, and δ_{H1}, δ_{H2}, δ_{H3} and δ_{H4} at 5.09, 4.15, 3.95 and 4.29 respectively, enabling the identification of a 5-α-Ara*f* unit, based on our previous studies with mycobacterial LAM [15]. Moreover, this was in agreement with the identification of 5-Ara*f* residues from the per-*O*-methylation analysis data. Spin systems IV and V, from the C-1 chemical shifts at δ 101.9 and δ 102.9 (IV_1 and V_1 respectively; Figure 3B), were tentatively assigned to β-Ara units, but the linkage mode of these β-Ara units could not be determined. Per-*O*-methylation analysis indicated the presence of 2-Ara*f* units, and so spin systems IV and/or V may correspond to 2-β-Ara*f* units.

The sequence of the main units was investigated by ^{1}H-^{13}C heteronuclear multiple bound correlation spectroscopy NMR experiments (results not shown). Correlation peaks were observed for spin systems I and II. H-1 of 2,5-α-Ara*f* (I_1) showed an intercyclic connectivity with their C-5 indicating that 2,5-α-Ara*f* were interconnected by ($\alpha 1 \rightarrow 5$) glycosidic linkages. In addition, H-1 of t-β-Ara*f* (II_1) correlated with C-2 of 2,5-α-Ara*f*, establishing that 2,5-α-Ara*f* were substituted at *O*-2 by t-β-Ara*f* residues. Taken together, these results demonstrate that

Table 1 Proton and carbon chemical shifts of AsuLAM

Chemical shifts were measured at 308 K in ^2H_2O and are referenced relative to internal acetone at δ_H 2.225 and δ_C 34.00. Abbreviation: n.d., not determined.

	Chemical shifts (p.p.m.)					
Residue	H-1 C-1	H-2 C-2	H-3 C-3	H-4 C-4	H-5/H-5′ C-5	H-6/H-6′ C-6
2,5-α-Ara*f* (I)	5.18 108.7	4.21 89.5	4.19 77.7	4.19 83.8	3.91/3.84 69.2	– –
t-β-Ara*f* (II)	5.15 103.4	4.16 79.1	4.07 77.0	3.92 84.8	3.81/3.70 65.8	– –
5-α-Ara*f* (III)	5.09 110.2	4.15 83.7	3.95 n.d.	4.29 n.d.	n.d. n.d.	– –
β-Ara*f* (IV)	5.30 101.9	4.31 83.2	n.d.	n.d.	n.d.	–
β-Ara*f* (V)	5.08 102.9	4.15 n.d.	n.d.	n.d.	n.d.	–
α-Man*p* (VI)	5.18 97.8	n.d.	n.d.	n.d.	n.d.	n.d.
α-Man*p* (VII)	5.15 97.8	n.d.	n.d.	n.d.	n.d.	n.d.
6-α-Man*p* (VIII)	4.91 n.d.	4.01 n.d.	n.d.	n.d.	n.d.	n.d.

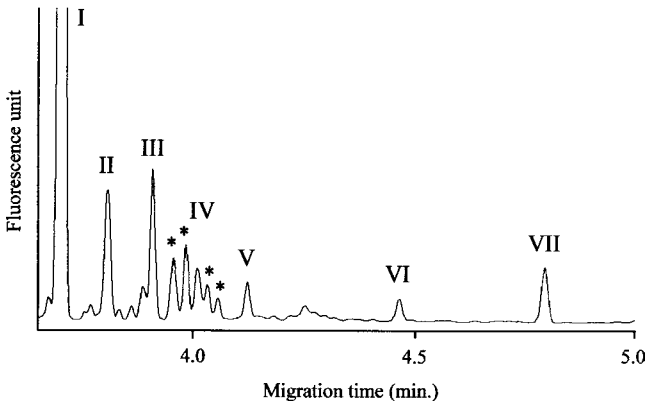

Figure 4 Partial electropherogram of oligosaccharide derivatives obtained by mild-acid-hydrolysed AsuLAM followed by APTS derivatization

AsuLAM (1 μg) and 0.1 nmol mannoheptose were hydrolysed with 15 μl of 0.1 M HCl for 20 min at 110 °C, dried and APTS derivatized. CE conditions were the same as in Figure 1. I, Ara-APTS; II, Man-APTS; III, internal standard, mannoheptose-APTS; IV, Araf-$\alpha(1 \rightarrow 5)$-Ara-APTS; V, Manp-Ara-APTS; VI, Manp-Manp-Ara-APTS; VII, Manp-Manp-Manp-Ara-APTS. Peaks labelled with asterisks could not be precisely attributed. One of them may correspond, according to the arabinan domain structure, to Araf-$\beta(1 \rightarrow 2)$-Ara-APTS.

the AsuLAM arabinan backbone is a multibranched structure composed of an $(\alpha 1 \rightarrow 5)$-Araf chain substituted at mostly the *O*-2 position by a single t-β-Araf unit. However, a minor proportion of the $(\alpha 1 \rightarrow 5)$-Araf backbone is not substituted, as shown by the identification of 5-α-Araf.

Mannan core and manno-oligosaccharide caps

CE-LIF and per-*O*-methylation analyses established the presence of Man residues. In mycobacterial ManLAM, Man residues are found either in the mannan core or in manno-oligosaccharide caps. In order to investigate the presence of manno-oligosaccharide caps, AsuLAM was partially hydrolysed using mild acid conditions (0.1M HCl for 30 min at 110 °C), APTS derivatized and subjected to CE-LIF analysis [37]. The electropherogram exhibited several peaks (Figure 4). Beside peaks corresponding to Ara-APTS (I), Man-APTS (II) and mannoheptose-APTS (III, internal standard), peaks IV, V, VI and VII had identical retention times to that of products obtained by mild acid hydrolysis of *M. bovis* BCG ManLAM (results not shown). Consequently, based on our previous studies with ManLAM [37], these peaks were assigned as Araf-Ara-APTS (IV), Manp-Ara-APTS (V), Manp-Manp-Ara-APTS (VI) and Manp-Manp-Manp-Ara-APTS (VII) (Figure 4). CE-LIF is a high resolution technique that allows the separation of oligosaccharide fragments differing only by their glycosidic linkage [37]. So the data obtained suggested that AsuLAM harboured the same manno-oligosaccharide caps as those observed in mycobacterial ManLAM, i.e. characterized by $(\alpha 1 \rightarrow 2)$ linkages. This was reinforced by the finding of 2-Manp and t-Manp residues in the per-*O*-methylation analysis. Peak IV indicated the presence of Araf-$(\alpha 1 \rightarrow 5)$-Ara units arising from the depolymerization of the arabinan domain. Peaks marked with an asterisk, with a migration time similar to compound IV, could not be precisely attributed (Figure 4). However, according to the arabinan domain determined above, one of the unknown peaks in Figure 4, could correspond to Araf-$(\beta 1 \rightarrow 2)$-Ara-APTS.

The relative abundance of each capping motif was determined using an internal standard. As a result AsuLAM was found to contain 1.1 mannose caps per molecule, with approximately 0.3 mono-mannosyl, 0.2 di-mannosyl and 0.6 tri-mannosyl units per molecule. The CE-LIF data suggested that the caps, as in mycobacterial ManLAM, substitute the arabinan segment at *O*-5, most probably the side-chain β-Araf units, suggesting the presence of 5-β-Araf residues. These residues are likely to correspond to the β-Araf units characterized by spin systems IV and/or V (Figure 3b).

Per-*O*-methylation analysis indicated the presence, albeit at low abundance, of 6-Manp, 2,6-Manp and 3,6-Manp, possibly representing a short $\alpha(1 \rightarrow 6)$ mannan domain, substituted at *O*-2 and *O*-3 positions. This was confirmed by detection of a ^{1}H NMR resonance, $VIII_1$, at δ_{H1} 4.91 (Figure 3a), which typifies 6-Manp units usually found in the mannan core of mycobacterial LAM [15,17]. The relatively low abundance confirms the short oligomerization of the mannan core. The NMR signature of the caps and mannan core units is unclear, nevertheless, the unassigned NMR spin systems VI and VII with δ_{C1} at 97.8 (VI_1 and VII_1, respectively; Figure 3B) can be assigned tentatively as 2-*O*-linked Manp residues [15,17]. C-1 resonances of t-α-Manp from both caps and the mannan core are found in mycobacterial LAM at around δ 104–105 [15] and may overlap here with the resonances of t-β-Araf units.

An integrated view of AsuLAM carbohydrate backbone

In summary, methylation, CE and NMR analyses allowed us to propose that the AsuLAM carbohydrate backbone contains a very short mannan domain consisting of an $(\alpha 1 \rightarrow 6)$-Manp chain, being occasionally substituted by t-α-Manp residues at *O*-2 or *O*-3. Attached to this short mannan domain is a multibranched arabinan domain composed of an $(\alpha 1 \rightarrow 5)$-Araf chain, the majority of which is substituted at *O*-2 by a single t-β-Araf unit. Some of these terminal residues may be further substituted at *O*-5 by $(\alpha 1 \rightarrow 2)$ oligomannosyl caps, with approximately one mannose-capping residue per molecule.

MPI anchor

Per-*O*-methylation analysis indicated the presence of a product which afforded in CI mode $(M + H)^+$ and $(M + NH_4)^+$ ions at *m*/*z* 321 and 338 respectively, characteristic of a di-acetylated, tetra-methylated inositol [38]. Electron impact mass spectrometry fragments at *m*/*z* 200, 191 and 75 allowed us to positively identify this compound as 2,6-diacetyl-1,3,4,5-tetramethyl-inositol [38,39]. These results strongly suggest that AsuLAM possesses a MPI anchor characterized by a diglycosylated *myo*-inositol unit substituted at positions 2 and 6, as established for mycobacterial LAM [8–10].

The structure of the MPI anchor was subsequently investigated by 1D ^{31}P and 2D ^{1}H-^{31}P NMR experiments [11,36]. The 1D ^{31}P spectrum of AsuLAM is dominated by a single resonance (results not shown). The proton resonances of the residues esterifying the phosphate were further assigned from 2D ^{1}H-^{31}P HMQC-HOHAHA NMR experiments (Figure 5). The phosphorus atom correlated with a set of proton signals that could be assigned to *myo*-inositol and glycerol protons (Figure 5 and Table 2). The assignments were further confirmed by 2D ^{1}H-^{31}P HMQC and ^{1}H-^{1}H HOHAHA NMR experiments (results not shown). According to the nomenclature used in our previous studies on LAM [11,36], we identified the phosphorus as P3, i.e. bearing a diacylglycerol unit and a non-acylated *myo*-inositol unit. The diacylated glycerol unit is typified by the presence of the deshielded H-2 proton at 5.1 p.p.m., whereas the H-3 resonance of the *myo*-inositol at 3.27 p.p.m. indicates that this position is not acylated. This

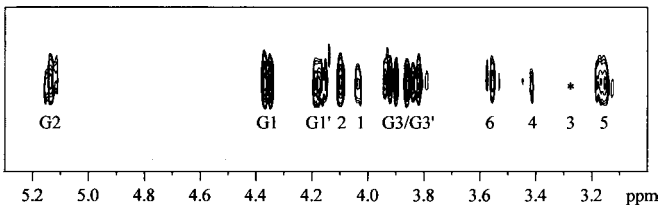

Figure 5 2D ^{1}H-^{31}P HMQC-HOHAHA τ_m 57 ms spectrum of AsuLAM in DMSO-*d*6 at 343 K

Expanded region (δ ^{31}P: 0.7-3.8, δ ^{1}H: 5.3-3.0) is shown. Numerals correspond to the proton number of the *myo*-inositol units and numerals with letter G, to the proton number of the glycerol units. Symbol (*) indicate a connectivity present on spectra but with weak intensity.

Table 2 *Myo*-inositol and glycerol proton chemical shifts

Chemical shifts were measured at 343 K in DMSO-*d*6 and are referenced relative to the internal DMSO signal at δ_H 2.52.

	Chemical shifts (p.p.m.)					
Residue	H-1(/H-1′)	H-2	H-3(/H-3′)	H-4	H-5	H-6
myo-inositol	4.03	4.10	3.27	3.41	3.16	3.56
glycerol	4.35/4.17	5.13	3.91/3.84	–	–	–

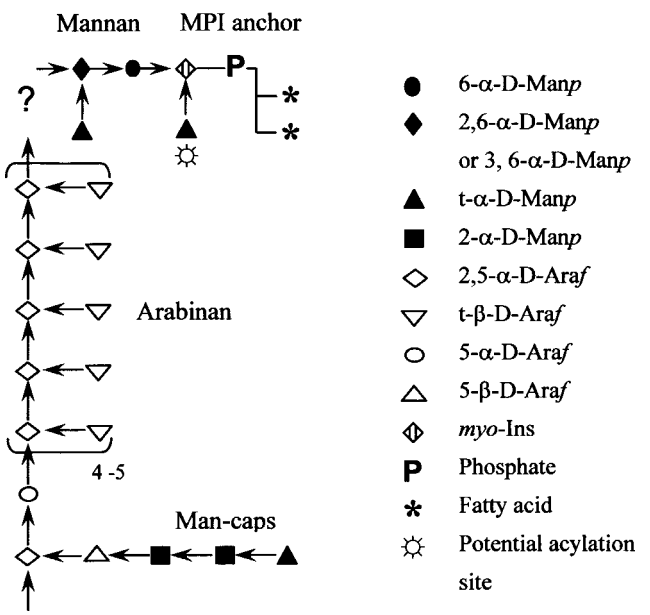

Scheme 1 Structural model of AsuLAM

AsuLAM contains 1.1 mannose caps per molecule, with approximately 0.3 mono-mannosyl, 0.2 di-mannosyl and 0.6 tri-mannosyl units per molecule. The major form, i.e. the trimannosylated one is drawn. 2-Ara*f* residues detected by per-*O*-methylation analysis could not be located on the structure.

strategy did not enable the investigation of the acylation state of position 6 of the Man*p* unit linked at *O*-2 to the *myo*-inositol unit, which has been described as a potential acylation site in mycobacterial LAM [8–10]. Altogether the structural analyses led us to propose the model depicted in Scheme 1.

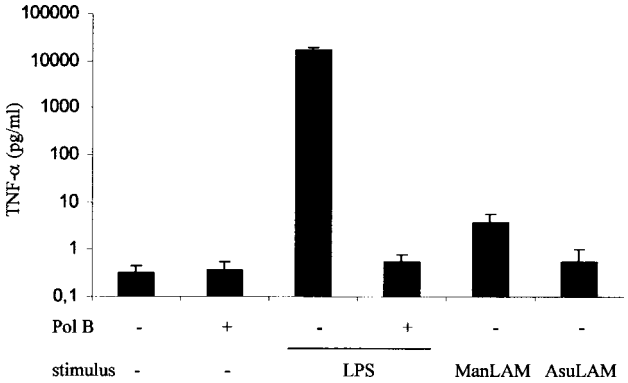

Figure 6 TNF-α production by J774 macrophages in response to various stimuli

Lipopolysaccharide (LPS) was tested at 0.2 μg/ml, whereas the different LAMs were tested at 10 μg/ml. One representative experiment out of three is shown. LPS was from *E. coli* 055:B5 (Sigma) and ManLAM from *M. bovis* BCG. Pol B, polymyxin B.

TNF-α production by macrophages

The potency of AsuLAM, in comparison with a mycobacterial ManLAM (from *M. bovis* BCG), to stimulate the production of TNF-α was investigated using murine (J774) and human (THP-1) macrophage cell lines. As expected, lipopolysaccharide, used as a positive control, induced a huge production of TNF-α by J774 macrophage cell lines (Figure 6). The production was completely abrogated by adding polymyxin B. AsuLAM, when tested at concentrations of 10 μg/ml (Figure 6) or 20 μg/ml (results not shown) was not able to significantly induce the production of TNF-α by J774 macrophage cell lines (Figure 6). Indeed, the amount of TNF-α elicited by AsuLAM was even less than that induced by *M. bovis* BCG ManLAM (Figure 6), which is already known to be a poor inducer of pro-inflammatory cytokines [17,21]. Identical results were obtained with THP-1 macrophage cell lines, except that the overall amount of TNF-α released in these experiments was weaker than that obtained with J774 cell lines (results not shown).

DISCUSSION

In the present study we have purified and characterized a novel LAM from *A. sulphurea*, now termed AsuLAM. Interestingly, AsuLAM was found by SDS/PAGE analysis to have a size intermediate between *M. tuberculosis* ManLAM (17 kDa) and LM (6 kDa) [8,9]. This was confirmed by MALDI-TOF-MS that provided an average molecular mass centred around 10 kDa. AsuLAM contained mainly Ara with a small amount of Man. Per-*O*-methylation and NMR analyses converged to establish the structure of the arabinan backbone as a multi-branched structure composed of (α1 $\rightarrow$ 5)-Ara*f* chains substituted predominantly at the *O*-2 position by a single t-β-Ara*f* unit (Scheme 1). The arabinan segment constitutes the major part of the molecule and its NMR signature is unambiguous. The arabinan domain is characterized by the presence of 2,5-α-Ara*f* units, identified, to our knowledge, for the first time in LAM-like molecules.

CE-LIF analysis of mild-acid-treated AsuLAM demonstrated that it also contained manno-oligosaccharide caps, similar in structure to those found in ManLAM from *M. tuberculosis* H37Rv and *M. bovis* BCG. Indeed the oligosaccharide caps recovered after mild acid hydrolysis and APTS tagging of AsuLAM co-injected with the corresponding structural elements obtained from *M. bovis* BCG ManLAM, indicated that they

may possibly have the same structure, i.e. mono- and $\alpha(1 \rightarrow 2)$-di- and tri-mannosides. The amount of each cap motif was determined to be 0.3, 0.2 and 0.6 per molecule, respectively, giving approximately one mannose capping motif per AsuLAM molecule. This is fewer than those observed for *M. bovis* BCG and *M. tuberculosis* H37Rv ManLAM where the dimannoside motif represents around 5 units per molecule with approximately 7 mannose capping motifs per molecule [37]. The occurrence of manno-oligosaccharide caps was supported by per-*O*-methylation analysis, which afforded t-Man*p* and 2-Man*p*, the constitutive units of the caps. The location of the caps is presumed to be at *O*-5 position of the β-Ara*f* residues, with approximately one β-Ara*f* unit per molecule being substituted by capping motifs. Due to the low abundance of these substituted β-Ara*f* and Man*p* capping residues, the NMR resonances are unclear; however, spin systems VI and VII may correspond to 2-*O*-linked Man*p* residues. The C-1 resonances of t-α-Man*p* may overlap with the resonances from t-β-Ara*f* units. Furthermore, spin systems IV and/or V are characteristic of β-Ara*f* units that are likely to correspond to the 5-β-Ara*f* residues determined through per-*O*-methylation. Per-*O*-methylation also revealed the presence of small amounts of 2-Ara*f* units that could not be located precisely on the structure. Also, linkage analysis data provided evidence for the existence of small amounts of 6-Man*p*, 2,6-Man*p* and 3,6-Man*p* units. The 6-α-Man*p* was unambiguously identified by its characteristic ^{1}H NMR resonance at δ 4.91 [15,17] (Figure 3A) and confirmed that these mannose residues were in very low abundance compared with the main structural elements of 2,5-α-Ara*f* and t-β-Ara*f*. The 6-Man*p*, 2,6-Man*p* and 3,6-Man*p* residues together with t-Man*p* residues are probably constitutive of a very short mannan core that is attached to the MPI anchor of AsuLAM.

The MPI anchor, through ^{31}P NMR analysis, was shown to be composed of only one acyl-form, in contrast to mycobacterial LAM that exhibit variations in the number and the position of the fatty acid residues [11,28,36]. Moreover, 2,6-diacetyl-1,3,4,5-tetramethyl-inositol could be identified by per-*O*-methylation analysis, suggesting that AsuLAM possesses a MPI anchor characterized by a diglycosylated *myo*-inositol unit substituted at positions *O*-2 and *O*-6 [8,9]. In addition, the diacylated glycerol (non-acylated inositol), characterized by 2D ^{1}H-^{31}P NMR experiments, typified, according to the mycobacterial LAM nomenclature, a phosphate P3. Interestingly the MPI anchor also contains as one of the main fatty acids, 14-methyl-pentadecanoate, a characteristic fatty acid of the *Amycolatopsis* genus [35]. Altogether the data propose an original structural model for AsuLAM (Scheme 1). The model exhibits the same global domains as described for mycobacterial ManLAM, but with some significant differences. Firstly, AsuLAM is smaller in size, mainly due to the much reduced mannan core and reduced capping motifs. Secondly, its arabinan domain, which is also slightly smaller, consists of a single branched chain as opposed to mycobacterial LAM that contains several lateral chains.

AsuLAM was not able to induce the production of TNF-α by human or by mouse macrophage cell lines. Its activity was even weaker than that observed for mycobacterial ManLAM, which is known to be a poor inducer of pro-inflammatory cytokines [18]. The ability of PILAM to induce the production of TNF-α has been attributed so far to the presence of phospho-inositol caps [17] and to its capacity to elicit TLR-2-dependent signalling in macrophages [40]. The present study provides an original mannose-capped LAM structure and reinforces the paradigm that, unlike PILAM, mannose-capped LAMs are poor inducers of pro-inflammatory cytokines, enabling the bacteria to avoid amplifying a pro-inflammatory cytokine response from the host immune system.

We gratefully acknowledge Mrs T. Brando and Mr J. D. Bounéry (Institut de Pharmacologie et de Biologie Structurale, Toulouse, France) for expert technical assistance with capillary electrophoresis and GLC-MS. GSB acknowledges support as a Lister Institute-Jenner Research Fellow. This work was supported by the Medical Research Council (G9901077 and G9901078) and the Wellcome Trust (058972).

REFERENCES

1 Gordon, R. E., Mishra, S. K. and Barnett, D. A. (1978) Some bits and pieces of the genus *Nocardia: N. carnea, N. vaccinii, N. transvalensis, N. orientalis and N. aerocolonigenes.* J. Gen. Microbiol. **109**, 69–78

2 Mishra, S. K., Gordon, R. E. and Barnett, D. A. (1980) Identification of nocardiae and streptomycetes of medical importance. J. Clin. Microbiol. **11**, 728–736

3 Tsuchida, T., Inuma, H., Kinoshita, N., Ikeda, T., Sawa, T., Hamada, M. and Takeuchi, T. (1995) Azicemicins A and B, a new antimicrobial agent produced by *Amycolatopsis*. I. Taxonomy, fermentation, isolation, characterization and biological activities. J. Antibiot. (Tokyo) **48**, 217–221

4 Matsumoto, N., Tsuchida, T., Umekita, M., Kinoshita, N., Iinuma, H., Sawa, T., Hamada, M. and Takeuchi, T. (1997) Epoxyquinomicins A, B, C and D, new antibiotics from *Amycolatopsis*. I. Taxonomy, fermentation, isolation and antimicrobial activities. J. Antibiot. (Tokyo) **50**, 900–905

5 Lechavalier, M. P., Prauser, H., Labeda, D. P. and Ruan, J. S. (1986) Two new genera of *Nocardioform actinomycetes: Amycolata gen*. nov. and *Amycolatopsis* gen. nov. Int. J. Syst. Bacteriol. **36**, 29–37

6 Goodfellow, M. (1987) The taxonomic status of *Rhodococcus equi*. Vet. Microbiol. **14**, 205–209

7 Brennan, P. J. and Nikaido, H. (1995) The envelope of mycobacteria. Annu. Rev. Biochem. **64**, 29–63

8 Vercellone, A., Nigou, J. and Puzo, G. (1998) Relationships between the structure and the roles of lipoarabinomannans and related glycoconjugates in tuberculosis pathogenesis. Front. Biosci. **3**, e149–e163

9 Chatterjee, D. and Khoo, K. H. (1998) Mycobacterial lipoarabinomannan: an extraordinary lipoheteroglycan with profound physiological effects. Glycobiology **8**, 113–120

10 Gilleron, M., Rivière, M. and Puzo, G. (2001) Roles of glycans in bacterial infections: interaction host-mycobacteria. In Glycans in cell interaction and recognition. Therapeutic aspects (Aubery, M., ed.), pp. 113–140, Harwood Academic Press, Amsterdam

11 Nigou, J., Gilleron, M. and Puzo, G. (1999) Lipoarabinomannans: characterization of the multiacylated forms of the phosphatidyl-myo-inositol anchor by NMR spectroscopy. Biochem. J. **337**, 453–460

12 Delmas, C., Gilleron, M., Brando, T., Vercellone, A., Gheorghui, M., Riviere, M. and Puzo, G. (1997) Comparative structural study of the mannosylated-lipoarabinomannans from *Mycobacterium bovis* BCG vaccine strains: characterization and localization of succinates. Glycobiology **7**, 811–817

13 Treumann, A., Xidong, F., McDonnell, L., Derrick, P. J., Ashcroft, A. E., Chatterjee, D. and Homans, S. W. (2002) 5-Methylthiopentose: a new substituent on lipoarabinomannan in *Mycobacterium tuberculosis* . J. Mol. Biol. **316**, 89–100

14 Chatterjee, D., Lowell, K., Rivoire, B., McNeil, M. R. and Brennan, P. J. (1992) Lipoarabinomannan of *Mycobacterium tuberculosis*. Capping with mannosyl residues in some strains. J. Biol. Chem. **267**, 6234–6239

15 Venisse, A., Berjeaud, J. M., Chaurand, P., Gilleron, M. and Puzo, G. (1993) Structural features of lipoarabinomannan from *Mycobacterium bovis* BCG. Determination of molecular mass by laser desorption mass spectrometry. J. Biol. Chem. **268**, 12401–12411

16 Khoo, K. H., Dell, A., Morris, H. R., Brennan, P. J. and Chatterjee, D. (1995) Inositol phosphate capping of the nonreducing termini of lipoarabinomannan from rapidly growing strains of *Mycobacterium*. J. Biol. Chem. **270**, 12380–12389

17 Gilleron, M., Himoudi, N., Adam, O., Constant, P., Venisse, A., Riviere, M. and Puzo, G. (1997) *Mycobacterium smegmatis* phosphoinositols-glyceroarabinomannans. Structure and localization of alkali-labile and alkali-stable phosphoinositides. J. Biol. Chem. **272**, 117–124

18 Nigou, J., Zelle-Rieser, C., Gilleron, M., Thurnher, M. and Puzo, G. (2001) Mannosylated lipoarabinomannans inhibit IL-12 production by human dendritic cells: evidence for a negative signal delivered through the mannose receptor. J. Immunol. **166**, 7477–7485

19 Knutson, K. L., Hmama, Z., Herrera-Velit, P., Rochford, R. and Reiner, N. E. (1998) Lipoarabinomannan of *Mycobacterium tuberculosis* promotes protein tyrosine dephosphorylation and inhibition of mitogen-activated protein kinase in human mononuclear phagocytes. Role of the Src homology 2 containing tyrosine phosphatase 1. J. Biol. Chem. **273**, 645–652

20 Adams, L. B., Fukutomi, Y. and Krahenbuhl, J. L. (1993) Regulation of murine macrophage effector functions by lipoarabinomannan from mycobacterial strains with different degrees of virulence. Infect. Immun. **61**, 4173–4181

21 Nigou, J., Gilleron, M., Rojas, M., Garcia, L. F., Thurnher, M. and Puzo, G. (2002) Mycobacterial lipoarabinomannans: modulators of dendritic cell function and the apoptotic response. Microbes. Infect. **4**, 945–953
22 Sutcliffe, I. C. (1995) Identification of a lipoarabinomannan-like lipoglycan in *Corynebacterium matruchotii*. Arch. Oral. Biol. **40**, 1119–1124
23 Sutcliffe, I. C. (2000) Characterization of a lipomannan lipoglycan from the mycolic acid containing actinomycete *Dietzia maris*. Antonie Van Leeuwenhoek **78**, 195–201
24 Flaherty, C. and Sutcliffe, I. C. (1999) Identification of a lipoarabinomannan-like lipoglycan in *Gordonia rubropertincta*. Syst. Appl. Microbiol. **22**, 530–533
25 Flaherty, C., Minnikin, D. E. and Sutcliffe, I. C. (1996) A chemotaxonomic study of the lipoglycans of *Rhodococcus rhodnii* N445 (NCIMB 11279). Zentralbl. Bakteriol. **285**, 11–19
26 Garton, N. J., Gilleron, M., Brando, T., Dan, H. H., Giguere, S., Puzo, G., Prescott, J. F. and Sutcliffe, I. C. (2002) A novel lipoarabinomannan from the equine pathogen *Rhodococcus equi*: structure and effect on macrophage cytokine production. J. Biol. Chem. **277**, 31722–31733
27 Nigou, J., Gilleron, M., Cahuzac, B., Bounery, J. D., Herold, M., Thurnher, M. and Puzo, G. (1997) The phosphatidyl-myo-inositol anchor of the lipoarabinomannans from *Mycobacterium bovis* bacillus Calmette Guerin. Heterogeneity, structure, and role in the regulation of cytokine secretion. J. Biol. Chem. **272**, 23094–23103
28 Ludwiczak, P., Gilleron, M., Bordat, Y., Martin, C., Gicquel, B. and Puzo, G. (2002) *Mycobacterium tuberculosis* phoP mutant: lipoarabinomannan molecular structure. Microbiology **148**, 3029–3037
29 Ciucanu, I. and Kerek, F. (1984) A simple and rapid method for the permethylation of carbohydrates. Carbohydr. Res. **131**, 209–217
30 Shaka, A. J., Barker, P. B. and Freeman, R. (1985) Computer-optimized decoupling scheme for wideband applications and low-level operation. J. Magn. Reson. **64**, 547–552
31 Bax, A. and Subramanian, S. (1986) Sensitivity-enhanced two-dimensional heteronuclear shift correlation NMR spectroscopy. J. Magn. Reson. **67**, 565–569
32 Lerner, L. and Bax, A. (1986) Sensitivity-enhanced two-dimensional heteronuclear relayed coherence transfer NMR spectroscopy. J. Magn. Reson. **69**, 375–380
33 Bax, A. and Davies, D. G. (1985) MLEV-17 based two-dimensional homonuclear magnetization transfer spectroscopy. J. Magn. Reson. **65**, 355–360
34 Espevik, T. and Nissen-Meyer, J. (1986) A highly sensitive cell line, WEHI 164 clone 13, for measuring cytotoxic factor/tumor necrosis factor from human monocytes. J. Immunol. Methods. **95**, 99–105
35 Lee, S. D. and Hah, Y. C. (2001) *Amycolatopsis albidoflavus* sp. nov. Int. J. Syst. Evol. Microbiol. **51**, 645–650
36 Gilleron, M., Bala, L., Brando, T., Vercellone, A. and Puzo, G. (2000) *Mycobacterium tuberculosis* H37Rv parietal and cellular lipoarabinomannans. Characterization of the acyl- and glyco-forms. J. Biol. Chem. **275**, 677–684
37 Nigou, J., Vercellone, A. and Puzo, G. (2000) New structural insights into the molecular deciphering of mycobacterial lipoglycan binding to C-type lectins: lipoarabinomannan glycoform characterization and quantification by capillary electrophoresis at the subnanomole level. J. Mol. Biol. **299**, 1353–1362
38 Chatterjee, D., Hunter, S. W., McNeil, M. and Brennan, P. J. (1992) Lipoarabinomannan. Multiglycosylated form of the mycobacterial mannosylphosphatidylinositols. J. Biol. Chem. **267**, 6228–6233
39 Guerardel, Y., Maes, E., Elass, E., Leroy, Y., Timmerman, P., Besra, G. S., Locht, C., Strecker, G. and Kremer, L. (2002) Structural study of lipomannan and lipoarabinomannan from *Mycobacterium chelonae*. Presence of unusual components with α1,3-mannopyranose side chains. J. Biol. Chem. **277**, 30635–30648
40 Means, T. K., Lien, E., Yoshimura, A., Wang, S., Golenbock, D. T. and Fenton, M. J. (1999) The CD14 ligands lipoarabinomannan and lipopolysaccharide differ in their requirement for Toll-like receptors. J. Immunol. **163**, 6748–6755

Received 3 February 2003/4 March 2003; accepted 6 March 2003
Published as BJ Immediate Publication 6 March 2003, DOI 10.1042/BJ20030197